Dalton Transactions

ROYAL SOCIETY OF CHEMISTRY

PAPER

View Article Online
View Journal

Cite this: DOI: 10.1039/d6dt00453a

CO_2 uptake potential of cerium(III) triazolates and tetrazolates

Jonas Riedmaier, Cäcilia Maichle-Mössmer and Reiner Anwander *

Cerous triazolates and tetrazolates were synthesised utilising $Ce[N(SiMe_3)_2]_3$ as a precursor. The transamination with $Htz^{Me,Me}$ ($tz^{Me,Me}$ = 3,5-dimethyl-1,2,4-triazolyl), $Htrz^{Bz}$ (trz^{Bz} = 1,2,3-benzotriazolyl) and $Htet^{Ph}$ (tet^{Ph} = 5-phenyltetrazolyl) gave insoluble, white solids, while $Htz^{Ph,Ph}$ ($tz^{Ph,Ph}$ = 3,5-diphenyl-1,2,4-triazolyl) led to the isolation of the monomeric complex $Ce(tz^{Ph,Ph})_3(thf)_3$. Triazolate $[Ce(tz^{Me,Me})_3]_n$ favoured exhaustive CO_2 insertion, while the less basic triazolate $[Ce(trz^{Bz})_3]_n$ and tetrazolate $[Ce(tet^{Ph})_3]_n$ displayed only partial and no insertion, respectively. $Ce(tz^{Ph,Ph})_3(thf)_3$ reacted with CO_2 in aromatic solvents but the product could not be identified. Addition of the azoles to $Ce[N(SiMe_3)_2]_3/Me_3TACN$ mixtures afforded discrete complexes $(Me_3TACN)Ce(az)_3(thf)$ (Me_3TACN = 1,4,7-trimethyl-1,4,7-triazacyclononane; az = $tz^{Me,Me}$, trz^{Bz}, tet^{Ph}), which, however, do not insert CO_2 at ambient temperature. Treatment of $(Me_3TACN)Ce(trz^{Bz})_3(thf)$ with CO_2 resulted in the separation of Me_3TACN and precipitation of a white powder. The respective pyrazolate $(Me_3TACN)Ce(pz^{Me,Me})_3$ ($pz^{Me,Me}$ = 3,5-dimethylpyrazolyl) featuring more basic azolato ligands engaged in CO_2 insertion, forming the previously reported complex $[Ce_4(pz^{Me,Me}{\cdot}CO_2)_{12}]$.

Received 22nd February 2026,
Accepted 26th March 2026

DOI: 10.1039/d6dt00453a

rsc.li/dalton

Introduction

The anthropogenic emission of greenhouse gases, especially carbon dioxide, is the main cause of global warming and the associated environmental impact and climate change.[1,2] Carbon capture and storage (CCS) and carbon capture and utilisation (CCU) are major strategies to curb the constantly increasing emissions.[3–6] Aqueous amines are currently employed on an industrial scale to chemically capture CO_2 by forming carbamates and/or ammonium bicarbonates.[7–9] This effective uptake process is based on the affinity of the nucleophilic nitrogen atoms to the electrophilic carbon centre of CO_2.[10,11] The oxophilic and Lewis acidic properties of rare-earth metals make the metal cations ideal electrophilic counterparts for the nucleophilic oxygen atoms. Such a synergistic Lewis acid base interaction was successfully targeted for the reversible insertion of CO_2 into homoleptic cerium dimethylpyrazolates, affording $Ce^{III}_4(pz^{Me,Me}{\cdot}CO_2)_{12}$ and $Ce^{IV}(pz^{Me,Me}{\cdot}CO_2)_4$ ($pz^{Me,Me}$ = 3,5-dimethylpyrazolyl).[12] We extended this approach to the light metals magnesium, aluminium, titanium, scandium and yttrium.[13–15]

The reversibility of CO_2 insertion into metal–ligand bonds can be assessed using the carboxophilicity criterion, which is strongly affected by the nucleophilicity of the ligand. To further study the impact of azolato bonding at the cerium(III) centre, we envisaged the more Brønsted-acidic triazoles and tetrazoles (pK_a(DMSO) = 19.8 (pyrazole), 14.8 (1,2,4-triazole), 13.9 (1,2,3-triazole), 11.9 (benzotriazole), 8.2 (tetrazole)).[16] Particular attention should be paid to homoleptic cerium tri- and tetrazolates and their capability of taking up CO_2. **Caution!** Great care must be taken when handling tetrazole derivatives which are classified as energetic materials due to their high nitrogen content.[17]

Reports on rare-earth-metal complexes containing anionic triazolato and tetrazolato ligands are very limited. The network compounds $[Eu_2(tz^{H,H})_5(Htz^{H,H})_2]^3_\infty$, $[Ho(tz^{H,H})_3(Htz^{H,H})_2]^2_\infty(Htz^{H,H})$ and $[Yb(tz^{H,H})_3]^3_\infty$ were obtained in a melt of parent 1,2,4-triazole ($Htz^{H,H}$) with Eu, Ho and Yb metals.[18,19] Additional examples include the monometallic lanthanum complex $La(tz^{Ph,Ph})_3(thf)_3$ [20] and several clusters with 1,2,4-triazolato ligands bearing pyridinyl or pyrazinyl substituents.[21,22] Likewise, the binary system lanthanide metal/1,2,3-triazole ($Htrz^{H,H}$) gave the frameworks $[Ln(trz^{H,H})_3]^{2-3}_\infty$ (Ln = La–Lu, except Eu) and $[Eu_3(trz^{H,H})_6(Htrz^{H,H})_2]^3_\infty$, respectively.[23–25] This chemistry was extended to 1,2,3-benzotriazole ($Htrz^{Bz}$), yielding $[Ln(trz^{Bz})_3(Htrz^{Bz})]^1_\infty$ (Ln = Ce, Pr).[26] The monometallic rare-earth-metal complex $LSc[NH(DIPP)](trz^{Ph,SiMe3})$ (L = [MeC{N(DIPP)}CHC(Me)(NCH$_2$CH$_2$N(Me)CH$_2$CH$_2$NMe$_2$)]$^-$, DIPP = 2,6-iPr$_2$C$_6$H$_3$) was synthesised by addition of benzonitrile to the nitrilimine $LSc[NH(DIPP)](N{=}N{=}CSiMe_3)$.[27] Analogously, $[Cp^*_2Ln\{CNN(SiMe_3)\}]_2$ (Ln = La, Sm; Cp* = pentamethyl-

Institut für Anorganische Chemie, Eberhard Karls Universität Tübingen, Auf der Morgenstelle 18, 72076 Tübingen, Germany.
E-mail: reiner.anwander@uni-tuebingen.de

cyclopentadienyl) reacted with pivalonitrile, forming $Cp^*_2Ln(trz^{SiMe_3,tBu})(NCtBu)$.[28] Recently, our group reported the isolation of the sandwich complexes $Cp^*_2Ce(tz^{Me,Me})(dmap)$ (dmap = *N*,*N*-dimethylpyridin-4-amine), $Cp^*_2Ce(tz^{Ph,Ph})(thf)_x$ (x = 0, 1) and $[Cp^*_2Ce(tet^{Ph})]_3$ (tet^{Ph} = 5-phenyltetrazolyl) and their reactivity towards CO_2.[29] Further rare-earth-metal tetrazolates include $LaL_3(H_2O)_3$ (L = 5-(2-pyridyl)tetrazolyl), synthesized by reacting $LaCl_3$, LH and Et_3N in H_2O,[30] and $Ln_2(bt)_3{\cdot}14H_2O$ (Ln = La, Ce; H_2bt = 5,5′-bitetrazole), obtained from a salt metathesis of $Ln_2(SO_4)_3$ and Ba(bt).[31]

Results and discussion

Cerium triazolates

In accordance with the synthesis of cerous pyrazolate $Ce_4(pz^{Me,Me})_{12}$,[32] our initial investigations towards a homoleptic cerium(III) triazolate were based on the protonolysis of $Ce[N(SiMe_3)_2]_3$ and three equiv. of 3,5-dimethyl-1,2,4-triazole ($Htz^{Me,Me}$) in benzene (Scheme 1). Due to the poor solubility of the triazole in non-donating solvents the reaction mixture was heated to 100 °C for three days. The resulting white powder **1** was amorphous and insoluble in aliphatic, aromatic or ethereal solvents including THF. This is most likely due to the formation of a polymeric species, since the 3,5-dimethylpyrazolato derivative forms tetrameric $Ce_4(pz^{Me,Me})_{12}$ in the solid state which is only sparingly soluble in toluene.[32] The ^{1}H NMR MAS (magic-angle spinning) spectrum of **1** shows one broad signal at −1.26 ppm for the methyl groups (Fig. S6). The carbon resonances in the ^{13}C HPDEC MAS spectrum (HPDEC = high power proton decoupling) appeared at 181.1 ppm for the carbon atoms in the 3- and 5-positions and at 11.5 ppm for the methyl groups (Fig. S7).

Exposing solid **1** to an atmosphere of 1 bar of CO_2 resulted in a mass gain of 22.3 wt% (5.06 mmol CO_2 g^{-1}) (Scheme 2). This corresponds to around 2.8 molecules of CO_2 per $[Ce(tz^{Me,Me})_3]$ unit, hence close to one CO_2 per triazolato ligand. For the implementation of solid-state NMR measurements of the amorphous $[Ce(tz^{Me,Me}{\cdot}CO_2)_3]_n$ (**1-CO$_2$**), the reaction was repeated employing labelled $^{13}CO_2$. The ^{1}H MAS NMR spectrum of $[Ce(tz^{Me,Me}{\cdot}{}^{13}CO_2)_3]_n$ (**1-^{13}CO$_2$**) exhibits two signals at 5.91 ppm and 1.26 ppm, assignable to the methyl groups of the triazolato ligand (Fig. S8). The ^{13}C HPDEC MAS spectrum shows two signals (Fig. S9). The signal at 161.0 ppm is ascribed to the inserted $^{13}CO_2$, overlaying the carbon resonance of the triazolato ring, while the methyl groups appeared at 6.5 ppm.

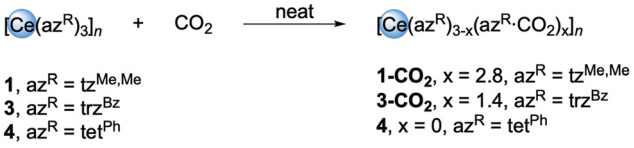

Scheme 2 Reaction of solid **1**, **3** and **4** with excess CO_2.

The CO_2 insertion is further corroborated by diffuse reflectance infrared Fourier transform spectroscopy (DRIFTS) of **1-CO$_2$**, which revealed bands at $\tilde{\nu}$ = 1753 cm^{-1} and $\tilde{\nu}$ = 1692 cm^{-1} assigned to the C=O stretching vibration (Fig. S31). A thermogravimetric analysis (TGA) of **1-CO$_2$** was performed in the range from 27 °C to 1050 °C (Fig. S39). A mass loss of 6% was observed between 27 °C and 110 °C, followed by another 11% between 110 °C and 370 °C. Then, a mass-loss event of 33% was detected between 370 °C and 550 °C. Unfortunately, none of these events can be assigned to a clear CO_2 loss, but the first two steps possibly include the loss of two molecules of CO_2 and perhaps the remaining solvent. The substantial mass loss in the third step indicates at least partial decomposition of the ligands.

We wondered whether substituting the Me groups with phenyl groups would increase the solubility of the formed complex. Accordingly, addition of three equiv. of $Htz^{Ph,Ph}$ to $Ce[N(SiMe_3)_2]_3$ in THF gave a colourless solution (Scheme 3). Cooling a CH_3CN/THF solution to −40 °C yielded colourless crystals of $Ce(tz^{Ph,Ph})_3(thf)_3$ (**2**). Performing the reaction in a non-donating solvent led to precipitation of a white solid. The ^{1}H NMR spectrum of **2** in C_6D_6 exhibits five signals, three for the phenyl protons and two for the coordinated THF (Fig. S10).

The solid-state structure of **2** is shown in Fig. 1, and is isostructural to the previously reported lanthanum derivative.[20] The coordination number of the cerium atom is nine, involving three κ^2 bonded triazolato ligands. Overall, the cerium centre adopts an octahedral coordination geometry with a facial arrangement of the six ligands. The Ce–N distances range from 2.4650(17) Å to 2.5535(16) Å (avg. 2.504 Å). As

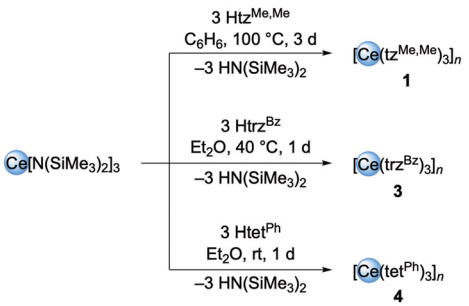

Scheme 1 Reaction of $Ce[N(SiMe_3)_2]_3$ with three equiv. of $Htz^{Me,Me}$, $Htrz^{Bz}$ and $Htet^{Ph}$ towards **1**, **3** and **4**, respectively.

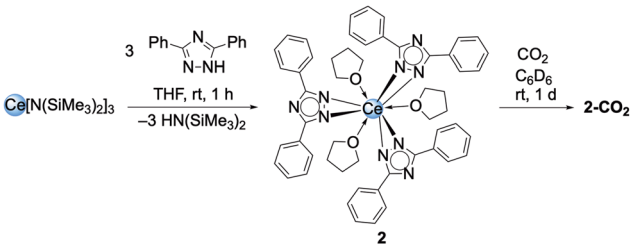

Scheme 3 Reaction of $Ce[N(SiMe_3)_2]_3$ with $Htz^{Ph,Ph}$ in THF to yield $Ce(tz^{Ph,Ph})_3(thf)_3$ (**2**) and reaction of **2** with CO_2 towards **2-CO$_2$**.

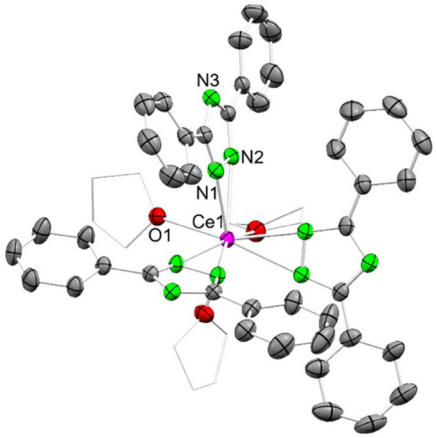

Fig. 1 Crystal structure of $Ce(tz^{Ph,Ph})_3(thf)_3$ (**2**). Ellipsoids are shown at a 50% probability level. Part of **2** is represented as a wireframe model. Hydrogen and disordered atoms are omitted for clarity. Selected interatomic distances/angles are listed in the SI.

expected, they are shorter than those in $La(tz^{Ph,Ph})_3(thf)_3$ (2.498(2) Å to 2.588(2) Å).[20] The respective pyrazolato congener $Ce(pz^{Ph,Ph})_3(thf)_3$ ($pz^{Ph,Ph}$ = 3,5-diphenylpyrazolyl) exhibits a similar average Ce–N distance of 2.507 Å,[33] but in contrast to **2** the ligands are arranged in a meridional fashion. For further comparison, the sandwich complexes $Cp^*_2Ce(tz^{Ph,Ph})$ and $Cp^*_2Ce(tz^{Ph,Ph})(thf)$ display Ce–N distances in the range of 2.4611 (15) Å to 2.4947(16) Å and 2.501(5) Å to 2.538(5) Å, respectively.[29] The Ce–O(thf) distances in **2** range from 2.5680(13) Å to 2.5773 (15) Å, which is on average shorter than those in the aforementioned THF adducts.

Exposing a C_6D_6 or toluene solution of **2** to an atmosphere of 1 bar of CO_2 afforded a slow colour change from colourless to bluish and – depending on the concentration – precipitation of a grey powder (**2-CO$_2$**, Scheme 3). The ^{1}H NMR spectrum of **2-CO$_2$** displayed seven signals which could not be assigned unequivocally (Fig. S12). A variable temperature (VT) NMR study did not show any re-formation of **2** at temperatures up to 80 °C under a CO_2 atmosphere (Fig. S13 and S14). NMR monitoring did not indicate any reaction of **2** with CO_2 in THF solution (Fig. S15). Consistent with that, the addition of THF to **2-CO$_2$** resulted in the re-formation of **2**. Applying vacuum to a toluene solution of **2-CO$_2$** or letting the grey powder dry under an argon atmosphere gave a white powder, which proved to be **2** by DRIFT spectroscopy. Exposing solid **2** to an atmosphere of 1 bar of CO_2 did not lead to any mass gain, which further lends evidence to our hypothesis that initial displacement of THF (in non-coordinating solvents) triggers the reaction with CO_2. Therefore, attempts to crystallise **2-CO$_2$** as well as the isolation of sufficient quantities for IR measurements and elemental analysis failed.

When applying a similar protonolysis protocol, the addition of three equiv. of $Htrz^{Bz}$ to $Ce[N(SiMe_3)_2]_3$ in Et_2O gave the white, insoluble powder **3** (Scheme 1). The insolubility possibly originates from the formation of polymeric $[Ce(trz^{Bz})_3]_n$, comparable to $[Ce(trz^{Bz})_3(Htrz^{Bz})]^1_\infty$ reported by the group of Müller-Buschbaum.[26] When exposing solid **3** to an atmosphere of 1 bar of CO_2, a mass gain of 10.9 wt% (2.47 mmol CO_2 g^{-1}) was detected. This matches 1.4 molecules of CO_2 per unit of **3**. Compared to that of $[Ce(trz^{Bz})_3]_n$ (**3**), the DRIFT spectrum of $[Ce(trz^{Bz})_{3-x}(trz^{Bz}{\cdot}CO_2)_x]_n$ (x = 1.4, **3-CO$_2$**) exhibits an additional band at $\tilde{\nu}$ = 1691 cm^{-1} (Fig. S34). The TGA revealed three mass loss events of 6%, 4% and 2% between 25 °C and 205 °C, 205 °C and 310 °C and 310 °C and 395 °C, respectively (Fig. S40). These amount to 12%, which is in the same range as the mass gain observed upon CO_2 uptake. Another mass loss of 13% was detected between 395 °C and 470 °C.

Cerium tetrazolates

To investigate any CO_2 uptake capacity of cerium(III) tetrazolates, 5-phenyltetrazole was chosen as a proligand. The reaction of $Ce[N(SiMe_3)_2]_3$ with three equiv. of $Htet^{Ph}$ in Et_2O yielded an insoluble, white powder (**4**, Scheme 1). In sharp contrast to the CO_2 uptake capability of the cerous triazolate complexes, solid **4** did not show any mass gain when put under a CO_2 atmosphere. The lack of CO_2 insertion was also corroborated by an unchanged IR spectrum. It can be assumed that the nucleophilicity of the tetrazolato ligand is not sufficient to favourably interact with CO_2 at ambient temperature. We would like to point out that heating **4** above 200 °C can lead to an explosive decomposition.

Azacrown-supported discrete cerous azolate complexes

To gain further insight into the cerium(III)–azolate bonding, the formation of monomeric complexes was targeted *via* the use of chelating donors. The neutral azacrown Me_3TACN (Me_3TACN = 1,4,7-trimethyl-1,4,7-triazacyclononane) seemed a promising candidate since it was successfully employed for the isolation of discrete methyl, halide and alkoxide complexes $(Me_3TACN)MX_3$ (M = Sc, X = Me, CH_2SiMe_3, Cl, OMe; M = Y, X = Me, CH_2SiMe_3, Cl, I, $OSi(OtBu)_3$; M = La, X = $CH_2C_6H_4$-4-Me; M = Tb, X = Cl; M = Yb, X = Me, Cl; M = Lu, X = Me) and several mixed ligand complexes.[34–47] A primary test regarding the interaction of $Ce[N(SiMe_3)_2]_3$ with Me_3TACN was run on an NMR-scale in C_6D_6 solution, resulting in partial precipitation of a solid. The ^{1}H NMR spectrum of the filtered solution showed three signals at 2.19, 1.90 and 1.67 ppm with an integral ratio of 9 : 6 : 6 in addition to free Me_3TACN, $Ce[N(SiMe_3)_2]_3$ and unknown signals (Fig. S16). This clearly indicates an interaction between $Ce[N(SiMe_3)_2]_3$ and Me_3TACN. Recently, the group of Evans addressed the question of THF coordination to $Ce[N(SiMe_3)_2]_3$.[48] Next, one equiv. of Me_3TACN was added to $Ce[N(SiMe_3)_2]_3$ in THF and stirred for 15 min followed by the addition of three equiv. of $Htz^{Me,Me}$ (Scheme 4). Crystallisation from THF resulted in colourless crystals of $(Me_3TACN)Ce(tz^{Me,Me})_3(thf)$ (**5**). The ^{1}H NMR spectrum shows only four signals, of which those at 6.15 ppm and 4.98 ppm can be assigned to the methyl groups of the azacrown and the triazolato ligands, respectively (Fig. S17). The NCH_2 protons of the azacrown appeared at 0.59 ppm and −3.48 ppm. It is plausible that the coordinated THF is displaced under reduced

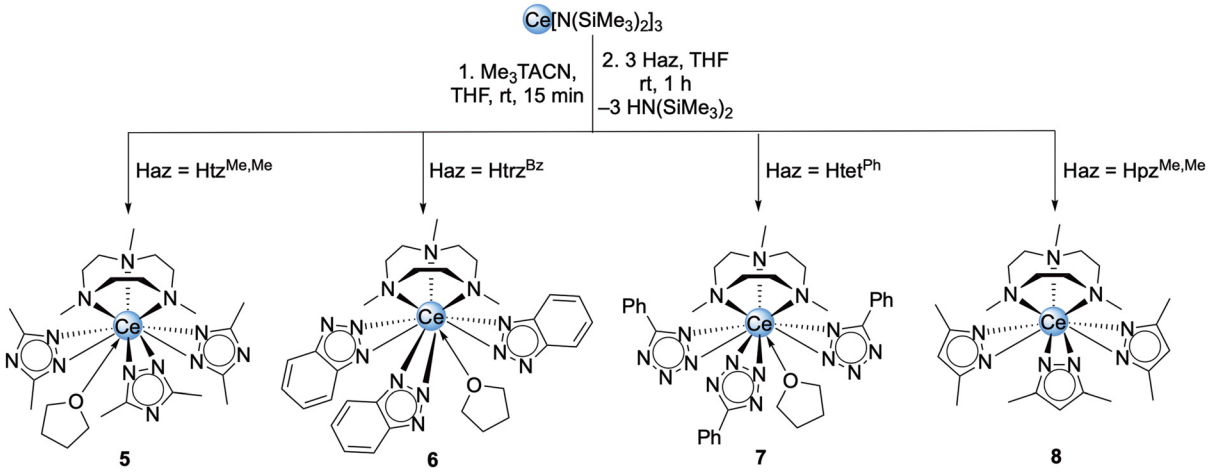

Scheme 4 Synthesis of complexes **5**, **6**, **7** and **8** *via* Me_3TACN-supported protonolysis of $Ce[N(SiMe_3)_2]_3$ with the respective proligands.

pressure, which is further supported by elemental analysis. Complex **5** crystallised in the space group $P2_1/n$. The 10-coordinate cerium centre adopts a distorted trigonal bipyramidal geometry (Fig. 2, left). The donor ligands Me_3TACN and THF occupy the axial positions, while the triazolato ligands occupy the equatorial ones. The cerium–nitrogen distances range from 2.5020(9) Å to 2.5985(9) Å for the triazolato ligands and from 2.7714(9) Å to 2.7975(9) Å for the azacrown. The Ce–O(thf) distance is 2.7259(8) Å. For comparison, 9-coordinate complex **2** has shorter Ce–N(triazolate) and C–O(thf) distances. The Ce–N distances of the three-dimensional framework structure of $[Ce(trz^{H,H})_3]^3_\infty$ featuring 9-cooordinate cerium centres as well are noted in the range of 2.37(3) Å to 2.70(3) Å (derived from Rietveld refinement).[23]

The benzotriazolate complex $(Me_3TACN)Ce(trz^{Bz})_3(thf)$ (**6**) can be accessed using the same protocol as applied for **5** (Scheme 4). However, the formation of large amounts of insoluble white powder was observed. Consequently, only a small number of crystals could be obtained from a THF solution. The ^{1}H NMR spectrum of **6** shows seven signals including the two peaks from THF (Fig. S19). The protons of the benzotriazolato ligand appear at 11.17 ppm and 8.63 ppm, respectively. Again, the NCH_3 protons appear at a higher field at 5.74 ppm in comparison with the NCH_2 protons which resonate at 0.85 ppm and −1.98 ppm. The ^{1}H NMR spectrum also revealed the presence of small signals of separated Me_3TACN, which increased significantly over several hours (Fig. S21), accompanied by the formation of a white solid. This indicates that **6** slowly decomposes to polymeric $[Ce(trz^{Bz})_3(thf)_x]_n$ species in THF, which also explains the low yield of the crystalline material.

Similar to the methyl-substituted triazolate derivative **5**, complex **6** crystallised in the space group $P2_1/c$ (Fig. 2, middle left). The ligand arrangement matches that of **5**, with the benzotriazolato ligands coordinating in a κ^2-fashion. The Ce–N (triazolato) distances are comparable to those detected for **5** and range from 2.529(2) Å to 2.587(8) Å. For further comparison, the coordination polymer $[Ce(trz^{Bz})_3(Htrz^{Bz})]^1_\infty$ exhibits Ce–N distances ranging from 2.521(9) Å to 2.653(8) Å.[26] The Ce–N(azacrown) distances (2.733(2)–2.765(2) Å) of complex **6** are in the range of those observed for **5**, but the Ce–O(thf) distance is significantly shorter (2.6693(19) Å).

In contrast to triazolate complex **6** the phenyltetrazolato congener $(Me_3TACN)Ce(tet^{Ph})_3(thf)$ (**7**) could be obtained in

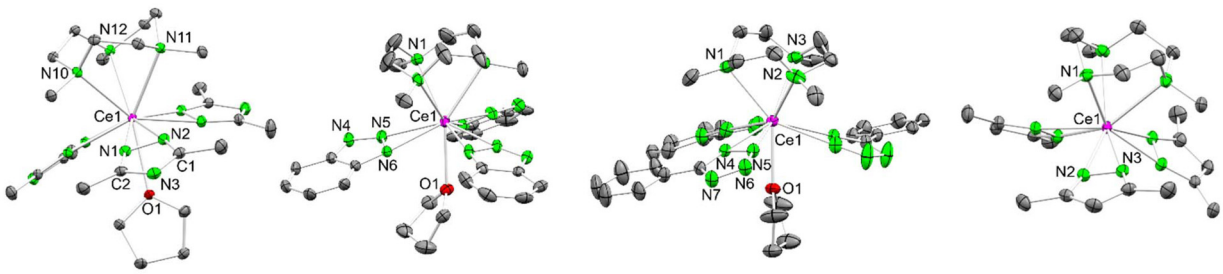

Fig. 2 Crystal structures of $(Me_3TACN)Ce(tz^{Me,Me})_3(thf)$ (**5**, left), $(Me_3TACN)Ce(trz^{Bz})_3(thf)$ (**6**, middle left), $(Me_3TACN)Ce(tet^{Ph})_3(thf)$ (**7**, middle right) and $(Me_3TACN)Ce(pz^{Me,Me})_3$ (**8**, right). Ellipsoids are shown at a 50% probability level. Disordered atoms for **6** and **7** are omitted for clarity. Hydrogen atoms are omitted for clarity. Selected interatomic distances/angles are listed in the SI.

high crystalline yield when employing the same reaction conditions (Scheme 4). Its ^{1}H NMR spectrum shows the phenyltetrazolato protons at 10.39 ppm, 8.06 ppm and 7.83 ppm (Fig. S22). The signal of the NCH_3 protons of the azacrown ligand overlaps with the THF signal, while the NCH_2 protons appear at 1.86 ppm and 1.65 ppm. The crystal structure of **7** is shown in Fig. 2 (middle right). Once again the five ligands form a distorted trigonal bipyramid with a κ^2-coordination of the azolato ligands. Interestingly, one phenyltetrazolato coordinates symmetrically *via* the nitrogen atoms in the 2- and 3-positions, while the other two coordinate asymmetrically involving the nitrogen atoms in the 1- and 2-positions. However, the respective Ce–N distances of 2.543(2)/2.599(2) Å and 2.5422(19) Å to 2.599(2) Å, respectively, are in the same range. When compared to the azolato metrics of the triazolate complexes **5** and **6**, the shortest Ce–N distance of **7** is longer, while the longest one is similar. The Ce–N(azacrown) distances of **7** range from 2.710(2) Å to 2.722(2) Å and the Ce–O(thf) distance amounts to 2.6322(18) Å.

For further comparison the Ce–N distance in the 8-coordinate azobis(tetrazolide) carbonate complex $[Ce_2(tetN{=}Ntet)_2(CO_3)(H_2O)_{10}]{\cdot}2\ H_2O$ was noted as 2.662(2) Å.[49] Unfortunately, none of the azacrown-supported complexes **5**, **6** and **7** engages in CO_2 insertion at 1 bar pressure.

We also wondered whether the azacrown would promote the formation of a monomeric 3,5-dimethylpyrazolate complex.[12] Therefore, by applying the same synthesis protocol, three equiv. of $Hpz^{Me,Me}$ were added to a preformed mixture of $Ce[N(SiMe_3)_2]_3$/Me_3TACN (Scheme 4). Crystallisation from THF yielded crystals of the composition $(Me_3TACN)Ce(pz^{Me,Me})_3$ (**8**). Differing from the aforementioned complexes, THF did not coordinate to the metal centre. The ^{1}H NMR spectrum in C_6D_6 exhibited the expected set of five signals (Fig. S24). The resonances at 9.16 ppm and 3.78 ppm displayed an integral ratio of 3 : 18, consistent with the ring protons and methyl groups of the $pz^{Me,Me}$ moieties. The NCH_2 groups appeared at 2.02 ppm and 0.75 ppm, while the NCH_3 groups of the azacrown were detected at 1.58 ppm. Noteworthily, addition of Me_3TACN to a solution of tetrameric $[Ce_4(pz^{Me,Me})_{12}]$ in THF-d_8 also gave access to monomeric complex **8** (Fig. S27). Complex **8** crystallised in the trigonal space group *R*3 featuring a 9-coordinate cerium centre (Fig. 2, right). The Ce–N(pyrazolato) distances were noted at 2.4675(18) Å and 2.5379(19) Å, which are on average shorter than those in 10-coordinate **5**. For further comparison, the donor-free $[Ce_4(pz^{Me,Me})_{12}]$, featuring two 10-, one 9- and one 8-coordinate cerium centre, exhibits Ce–N(pyrazolato) distances in the range from 2.368(4) Å to 3.077(4) Å.[32] The Ce–N(azacrown) distances of **8** are 2.751(2) Å.

Reacting pyrazolate complex **8** with CO_2 in C_6D_6 or toluene-d_8 resulted in the disappearance of the NMR signals of the starting material (Fig. S29). The ^{1}H NMR spectra revealed the release of Me_3TACN as well as peaks assigned to $[Ce_4(pz^{Me,Me}{\cdot}CO_2)_{12}]$.[12] Consequently, there is exhaustive insertion of CO_2 into **8**, affording the same insertion product as for the homoleptic pyrazolate complex $[Ce_4(pz^{Me,Me})_{12}]$. Moreover, the CO_2 insertion seems to outperform azacrown coordination at cerium pyrazolate complexes.

Electronic absorption spectra

In THF solution, the triazolate complex **2** shows two absorption maxima at 236 nm and 266 nm (Fig. S41). The azacrown-supported triazolato and pyrazolato complexes **5** and **8** feature growing absorption until the cutoff wavelength of the solvent (Fig. S42 and S44). The global absorption maximum of **7** is detected at 243 nm (Fig. S43).

Conclusions

Homoleptic cerium(III) tri- and tetrazolates are easily accessible *via* protonolysis of $Ce[N(SiMe_3)_2]_3$ with the respective azoles, affording white powders insoluble in common organic solvents. The solids can chemisorb CO_2 at atmospheric pressure depending on the basicity of the azolato ligand. The 1,2,4-triazolate $[Ce(tz^{Me,Me})_3]_n$ showed near exhaustive CO_2 insertion, while the 1,2,3-triazolate $[Ce(trz^{Bz})_3]_n$ inserted 1.4 molecules of CO_2 per monomeric unit. Solid tetrazolate $[Ce(tet^{Ph})_3]_n$ featuring the least basic azolato ligand did not react with CO_2 under the prevailing conditions. The $Htz^{Ph,Ph}$ proligand also gave access to soluble triazolate complex $Ce(tz^{Ph,Ph})_3(thf)_3$, which revealed a CO_2 reaction in aromatic solvents.

Utilising the tridentate azacrown Me_3TACN in the protonolysis mixtures favoured the isolation of the monomeric complexes $(Me_3TACN)Ce(tz^{Me,Me})_3(thf)$, $(Me_3TACN)Ce(trz^{Bz})_3(thf)$ and $(Me_3TACN)Ce(tet^{Ph})_3(thf)$. While none of these complexes showed CO_2 insertion under ambient conditions, the corresponding pyrazolato complex, $(Me_3TACN)Ce(pz^{Me,Me})_3$, did. Treatment of this complex with CO_2 resulted in the loss of the Me_3TACN donor ligand and the formation of tetrameric $[Ce_4(pz^{Me,Me}{\cdot}CO_2)_{12}]$. This behaviour corroborates our hypothesis that the most basic cerous azolates favour CO_2 insertion into the Ce–N(azolato) bond, even in the presence of a chelating donor such as azacrowns. The respective complexes with less nucleophilic tri- and tetrazolato ligands do not react with CO_2 under ambient conditions. The present study might also give some valuable molecular insights into rare-earth-metal–azolate framework structures which are currently employed for CCS and CCU applications.[50–53]

Experimental

General considerations

Caution: 5-Phenyltetrazole is an energetic compound with sensitivity towards heat. Although at temperatures below 200 °C we did not face any problems, 5-phenyltetrazole and derivatives thereof should be handled with care, especially when larger quantities are required. All reactions were performed under an inert atmosphere (Ar) by using a glovebox (MBraun UNIlab^{pro}; <0.1 ppm O_2, <0.1 ppm H_2O) or according to standard Schlenk techniques in oven-dried glassware. Unless

otherwise stated, the solvents were purified with Grubbs-type columns (MBraun SPS, solvent purification system) and stored in a glovebox. Benzene was dried by refluxing with Na followed by distillation. CO_2 was purchased from Westfalen AG. Anhydrous cerium(III) chloride (99.5%) was purchased from abcr and activated *via* Soxhlet extraction with THF, giving $CeCl_3(thf)$. C_6D_6 and THF-d_8 were purchased from Sigma Aldrich and dried over NaK alloy. C_6D_6 and THF-d_8 were filtered and stored in a glovebox. THF-d_8 was also stored over molecular sieves (3 Å). 3,5-Dimethyltriazole and 5-phenyltetrazole were purchased from TCI. Benzotriazole and potassium bis(trimethylsilyl)amide were purchased from Sigma Aldrich. 1,4,7-Trimethyl-1,4,7-triazacyclononane was purchased from abcr. $Ce[N(SiMe_3)_2]_3$ was synthesised according to a modified published procedure utilising $KN(SiMe_3)_2$.[54]

NMR spectra were recorded on a Bruker AVII+400 (^{1}H: 400.11 MHz, ^{13}C: 100.61 MHz) or a Bruker AVII+500 (^{1}H: 500.13 MHz) at 26 °C using J. Young-valved NMR tubes. Solid-state NMR spectra were recorded on a Bruker AVIIIHD-300WB (^{1}H: 300.13 MHz, ^{13}C: 75.47 MHz) using a ZrO_2 rotor (4 mm diameter). ^{13}C MAS spectra were recorded utilizing high power proton decoupling (HPDEC). ^{1}H and ^{13}C NMR chemical shifts are referenced to a solvent resonance and reported in parts per million (ppm) relative to tetramethylsilane. Analysis of the NMR spectra was performed with TopSpin 3.6.0 and ACD/NMR Processor Academic Edition (product version: 12.01). Multiplicities of signals are given as singlet (s), doublet (d), triplet (t) and multiplet (m). DRIFT spectra were recorded on a Bruker INVENIO R spectrometer and converted using the Kubelka–Munk refinement. The samples were mixed with KBr and measured in a cell with KBr windows. Elemental analysis (C, H, N) was performed on a Elementar vario MICRO cube. Absorption measurements were performed on a PerkinElmer Lambda 35 spectrometer. Crystals for X-ray crystallography were handpicked in a glovebox, coated with Parabar 10312 and stored on microscope slides. Crystallographic data were collected on a Bruker APEX II DUO diffractometer by using QUAZAR optics and Mo K_α radiation (λ = 0.71073 Å). The data collection strategy was determined using COSMO[55] employing φ and ω scans. Raw data were processed using APEX3 [56] and SAINT.[57] Corrections for absorption effects were applied using SADABS.[58] The structures were solved using direct methods and refined against F^2 using SHELXTL[59,60] and Shelxl.[61] Disorder models were calculated using DSR,[61] a program included in ShelXle.[62] All graphics were produced employing Mercury[63] and POV-Ray.[64]

Syntheses

$[Ce(tz^{Me,Me})_3]_n$ (1). $Ce[N(SiMe_3)_2]_3$ (621 mg, 1.00 mmol, 1.00 equiv.) in benzene (10 mL) was added to $Htz^{Me,Me}$ (291 mg, 3.00 mmol, 3.00 equiv.) in benzene (5 mL) in a pressure tube and heated to 100 °C for 3 days, resulting in a white suspension. The mixture was centrifuged and washed with benzene (2 × 5 mL) and the residual solvent was removed under reduced pressure. An off-white powder was obtained (381 mg, 0.889 mmol, 89%). ^{1}H MAS NMR (300.1 MHz, 26 °C, MAS at 8 kHz): δ = −1.26 (tz-CH_3) ppm. ^{13}C MAS NMR (75.5 MHz, 24 °C, MAS at 8 kHz): δ = 181.1 (tz-NC), 11.5 (tz-CH_3) ppm. DRIFT: $\tilde{\nu}$ = 2968 (w), 2931 (w), 1513 (s), 1479 (s), 1412 (vs), 1365 (m), 1308 (m), 1042 (vw), 1007 (vw), 976 (w), 747 (m), 699 (w) 617 (w), 454 (vw) cm^{-1}. Elemental analysis (%) calcd for $C_{12}H_{18}CeN_9$ (428.46 g mol^{-1}): C 33.64, H 4.23, N 29.42; found: C 34.95, H 4.26, N 28.13. Although the results are outside the range viewed as establishing analytical purity (C +1.31%, N −1.29%), they are provided to illustrate the best values obtained to date.

$[Ce(tz^{Me,Me}{\cdot}CO_2)_3]_n$ (1-CO_2). A Schlenk tube was loaded with solid $[Ce(tz^{Me,Me})_3]_n$ (107 mg, 250 µmol), and the atmosphere was exchanged with 1 bar CO_2, which was maintained during the reaction time. After 18 h **1-CO_2** could be collected as a white powder (138 mg). ^{1}H MAS NMR (300.1 MHz, 24 °C, MAS at 8 kHz): δ = 5.91 (tz-CH_3), 1.26 (tz-CH_3) ppm. ^{13}C MAS NMR (75.5 MHz, 25 °C, MAS at 8 kHz): δ = 161.0 (NCO_2, tz-NC), 6.5 (tz-CH_3) ppm. DRIFT: $\tilde{\nu}$ = 2970 (w), 2932 (w), 1753 (m), 1692 (s), 1631 (vw), 1586 (w), 1513 (s), 1479 (s), 1444 (s), 1412 (vs), 1365 (s), 1308 (vs), 1147 (w), 1044 (w), 1008 (m), 976 (m), 841 (w), 790 (w), 766 (m), 748 (m), 699 (m), 617 (m), 500 (vw), 452 (w) cm^{-1}. Elemental analysis calcd for $C_{14.8}H_{18}CeN_9O_{5.6}$ (551.68 g mol^{-1}): C 32.22, H 3.29, N 22.85; found: C 33.62, H 4.21, N 24.72. The results are outside the range viewed as establishing analytical purity (C +1.40%, H +0.92%, N +1.87%). This could be due to residual solvent and/or loss of CO_2 under an argon atmosphere.

$Ce(tz^{Ph,Ph})_3(thf)_3$ (2). $Ce[N(SiMe_3)_2]_3$ (124 mg, 200 µmol, 1.00 equiv.) in THF (3 mL) was added dropwise to $Htz^{Ph,Ph}$ (133 mg, 600 µmol, 3.00 equiv.) in THF (2 mL) and stirred for 1 h. Then all volatile compounds were removed, giving an off-white powder. Crystallisation from *n*-hexane/THF at −40 °C yielded colourless crystals of **2** (173 mg, 170 µmol, 85%). ^{1}H NMR (C_6D_6, 400.1 MHz, 26 °C): δ = 12.32 (12H, s, *ortho*-C*H*), 8.16 (12H, s, *meta*-C*H*), 7.84 (6H, s, *para*-C*H*), −1.32 (12H, s, thf-CH_2), −2.15 (12H, s, thf-OCH_2) ppm. ^{13}C{^{1}H} NMR (C_6D_6, 100.6 MHz, 26 °C): δ = 183.7 (tz-N*C*), 137.3 (*ipso-C*), 130.6 (*meta-C*), 129.3 (*para-C*), 58.1 (thf-O*C*H$_2$), 22.0 (thf-*C*H$_2$) ppm. The signal of the *ortho* carbon could be detected, possibly due to overlap with the solvent signal. DRIFT: $\tilde{\nu}$ = 3062 (m), 2982 (m), 2888 (m), 1605 (w), 1467 (vs), 1426 (vs), 1402 (s), 1285 (m), 1175 (m), 1069 (m), 1025 (s), 992 (m), 922 (m), 869 (s), 790 (m), 730 (vs), 696 (vs), 553 (vw), 490 (vw), 422 (m) cm^{-1}. Elemental analysis (%) calcd for $C_{54}H_{54}CeN_9O_3$ (1017.20 g mol^{-1}): C 63.76, H 5.35, N 12.39; found: C 63.62, H 5.55, N 11.85. Although the results are outside the range viewed as establishing analytical purity (N −0.54%), they are provided to illustrate the best values obtained to date.

$[Ce(trz^{Bz})_3]_n$ (3). $Htrz^{Bz}$ (179 mg, 1.50 mmol, 3.00 equiv.) in Et_2O (7 mL) was added dropwise to $Ce[N(SiMe_3)_2]_3$ (311 mg, 0.500 mmol, 1.00 equiv.) in Et_2O (3 mL), resulting in the precipitation of a white solid. The resulting slurry was stirred at 40 °C for 1 d. The reaction mixture was centrifuged and washed with Et_2O (5 mL) and the residual solvent was removed under reduced pressure. An off-white powder was obtained (228 mg, 461 µmol, 92%). DRIFT: $\tilde{\nu}$ = 3052 (w), 1574 (w), 1485 (w), 1443 (m), 1390 (vw), 1283 (s), 1259 (m), 1174 (m),

1149 (m), 989 (w), 939 (vw), 914 (m), 848 (w), 782 (vs), 745 (vs), 694 (m), 633 (s), 551 (s), 433 (w) cm^{-1}. Elemental analysis (%) calcd for $C_{18}H_{12}CeN_9$ (494.47 g mol^{-1}): C 43.72, H 2.45, N 25.49; found: C 44.72, H 2.48, N 25.09. Although the results are outside the range viewed as establishing analytical purity (C +1.00%), they are provided to illustrate the best values obtained to date.

$[Ce(trz^{Bz}{\cdot}CO_2)_3]_n$ (3-CO_2). A Schlenk tube was loaded with solid **3** (124 mg, 250 μmol), and the atmosphere was exchanged with 1 bar CO_2, which was maintained during the reaction time. After 18 h **3-CO_2** could be collected as a white powder (139 mg). DRIFT: $\tilde{\nu}$ = 3052 (w), 1691 (w), 1574 (w), 1486 (m), 1444 (m), 1390 (w), 1284 (s), 1145 (s), 989 (w), 914 (s), 845 (w), 782 (vs), 746 (vs), 694 (m), 633 (s), 551 (s), 434 (m) cm^{-1}. Elemental analysis calcd for $C_{19.4}H_{12}CeN_9O_{2.8}$ (556.09 g mol^{-1}): C 41.90, H 2.18, N 22.67; found: C 43.81, H 2.64, N 23.94. Although the results are outside the range viewed as establishing analytical purity (C +1.91%, N +1.27%), they are provided to illustrate the best values obtained to date.

$[Ce(tet^{Ph})_3]_n$ (4). $Htet^{Ph}$ (219 mg, 1.50 mmol, 3.00 equiv.) in Et_2O (7 mL) was added dropwise to $Ce[N(SiMe_3)_2]_3$ (311 mg, 0.500 mmol, 1.00 equiv.) in Et_2O (3 mL). The reaction mixture was stirred for 1 d, resulting in a white suspension. The mixture was centrifuged and washed with Et_2O (5 mL) and the residual solvent was removed under reduced pressure. An off-white powder was obtained (271 mg, 0.471 mmol, 94%). DRIFT: $\tilde{\nu}$ = 3065 (w), 1525 (w), 1449 (vs), 1358 (m), 1281 (w), 1161 (w), 1143 (w), 1073 (w), 1010 (m), 922 (w), 846 (vw), 786 (m), 730 (vs), 693 (vs), 509 (w), 462 (w) cm^{-1}. Elemental analysis (%) calcd for $C_{21}H_{15}CeN_{12}$ (575.55 g mol^{-1}): C 43.82, H 2.63, N 29.20; found: C 43.92, H 2.71, N 28.59. Although the results are outside the range viewed as establishing analytical purity (N −0.61%), they are provided to illustrate the best values obtained to date.

Reaction of $[Ce(tet^{Ph})_3]_n$ with CO_2. A Schlenk tube was loaded with solid **4**, and the atmosphere was exchanged with 1 bar CO_2, which was maintained during the reaction time. After 18 h a white powder could be collected, which proved to be **4**.

Reaction of $Ce[N(SiMe_3)_2]_3$ with Me_3TACN. $Ce[N(SiMe_3)_2]_3$ (18.6 mg, 30.0 μmol, 1.00 equiv.) in C_6D_6 (0.3 mL) and Me_3TACN (5.1 mg, 30 μmol, 1.0 equiv.) in C_6D_6 (0.2 mL) were placed in a J. Young NMR tube, resulting in the slow precipitation of a solid. The solution was filtered before NMR measurement (Fig. S16).

$(Me_3TACN)Ce(tz^{Me,Me})_3(thf)$ (5). Me_3TACN (34.3 mg, 200 μmol, 1.00 equiv.) in THF (1 mL) was added dropwise to $Ce[N(SiMe_3)_2]_3$ (124 mg, 200 μmol, 1.00 equiv.) in THF (1 mL) and stirred for 15 min. Then, $Htz^{Me,Me}$ (58.3 mg, 600 μmol, 3.00 equiv.) in THF (4 mL) was added dropwise whereby the solution became slightly cloudy. After stirring the mixture for 1 h, all volatile compounds were removed, resulting in a white solid. Crystallisation from THF at −40 °C yielded colourless crystals of **5** (75.1 mg, 125 μmol, 63% yield without coordinated THF). ^1H NMR (THF-d_8, 400.1 MHz, 26 °C): δ = 6.15 (9H, s, NCH_3), 4.98 (18H, s, tz-CH_3), 0.59 (6H, s, NCH_2), −3.48 (6H, s, NCH_2) ppm. $^{13}C\{^1H\}$ NMR (THF-d_8, 100.6 MHz, 26 °C): δ = 176.4 (tz-N*C*), 42.5 (N*C*H_3), 38.9 (N*C*H_2), 17.9 (tz-*C*H_3) ppm. DRIFT: $\tilde{\nu}$ = 2982 (m), 2922 (m), 2862 (m), 2817 (m), 1483 (s), 1461 (vs), 1416 (vs), 1365 (m), 1301 (s), 1207 (w), 1150 (w), 1076 (s), 1043 (w), 1008 (s), 889 (w), 766 (m), 745 (s), 619 (m), 576 (w), 423 (m) cm^{-1}. Elemental analysis (%) calcd for $C_{21}H_{39}CeN_{12}$ (599.74 g mol^{-1}) (without THF): C 42.06, H 6.55, N 28.03; found: C 42.18, H 6.35, N 28.05.

$(Me_3TACN)Ce(trz^{Bz})_3(thf)$ (6). Me_3TACN (34.3 mg, 200 μmol, 1.00 equiv.) in THF (1 mL) was added dropwise to $Ce[N(SiMe_3)_2]_3$ (124 mg, 200 μmol, 1.00 equiv.) in THF (1 mL) and stirred for 15 min. Then, $Htrz^{Bz}$ (71.5 mg, 600 μmol, 3.00 equiv.) in THF (4 mL) was added dropwise. After stirring the mixture for 1 h, all volatile compounds were removed, resulting in a white solid. Crystallisation from THF at −40 °C yielded colourless crystals of **6** (5.8 mg, 8.7 μmol, 4%). ^1H NMR (THF-d_8, 400.1 MHz, 26 °C): δ = 11.17 (6H, s, trz-C*H*), 8.63 (6H, s, trz-C*H*), 5.74 (9H, s, NCH_3), 3.62 (4H, m, thf-OCH_2), 1.78 (4H, m, thf-CH_2), 0.85 (6H, s, NCH_2), −1.98 (6H, s, NCH_2) ppm. $^{13}C\{^1H\}$ NMR (THF-d_8, 100.6 MHz, 26 °C): δ = 163.7 (trz-N*C*), 125.4 (trz-*C*), 121.9 (trz-*C*), 68.0 (thf-O*C*H_2), 43.8 (N*C*H_3), 40.7 (N*C*H_2), 26.2 (thf-*C*H_2) ppm.

$(Me_3TACN)Ce(tet^{Ph})_3(thf)$ (7). Me_3TACN (34.3 mg, 200 μmol, 1.00 equiv.) in THF (1 mL) was added dropwise to $Ce[N(SiMe_3)_2]_3$ (124 mg, 200 μmol, 1.00 equiv.) in THF (1 mL) and stirred for 15 min. Then, $Htet^{Ph}$ (87.7 mg, 600 μmol, 3.00 equiv.) in THF (4 mL) was added dropwise whereby the solution became slightly cloudy. After stirring the mixture for 1 h, all volatile compounds were removed, resulting in a white solid. Crystallisation from THF at −40 °C yielded colourless crystals of **7** (145 mg, 177 μmol, 88%). ^1H NMR (THF-d_8, 400.1 MHz, 26 °C): δ = 10.39 (6H, d, *ortho*-C*H*), 8.06 (6H, t, *meta*-C*H*), 7.83 (3H, t, *para*-C*H*), 3.62 (13H, m, NCH_3 and thf-OCH_2), 1.86 (6H, s, NCH_2), 1.78 (4H, m, thf-CH_2), 1.65 (6H, s, NCH_2) ppm. $^{13}C\{^1H\}$ NMR (THF-d_8, 100.6 MHz, 26 °C): δ = 174.8 (tet-N*C*), 132.4 (*ipso-C*), 130.3 (*meta-C*), 130.0 (*para-C*), 128.9 (*ortho-C*), 68.0 (thf-O*C*H_2), 45.2 (N*C*H_2), 42.8 (N*C*H_3), 26.2 (thf-*C*H_2) ppm. DRIFT: $\tilde{\nu}$ = 3063 (w), 2981 (m), 2869 (m), 1494 (w), 1444 (s), 1358 (m), 1279 (w), 1204 (w), 1151 (m), 1114 (m), 1073 (s), 1029 (m), 1005 (s), 924 (w), 883 (m), 790 (m), 769 (m), 735 (vs), 698 (s), 579 (w), 511 (w), 461 (w), 425 (w) cm^{-1}. Elemental analysis (%) calcd for $C_{25}H_{47}CeN_{12}O$ (671.85 g mol^{-1}): C 44.69, H 7.05, N 25.02; found: C 49.78, H 5.29, N 24.43. Although the results are outside the range viewed as establishing analytical purity (C +5.09%, H −1.76%, N −0.59%), they are provided to illustrate the best values obtained to date. This could be due to incomplete combustion.

$(Me_3TACN)Ce(pz^{Me,Me})_3$ (8). Me_3TACN (34.3 mg, 200 μmol, 1.00 equiv.) in THF (1 mL) was added dropwise to $Ce[N(SiMe_3)_2]_3$ (124 mg, 200 μmol, 1.00 equiv.) in THF (1 mL) and stirred for 15 min. Then, $Hpz^{Me,Me}$ (57.7 mg, 600 μmol, 3.00 equiv.) in THF (4 mL) was added dropwise and the mixture was stirred for 2 h. After removal of all volatile compounds a white solid was obtained. Crystallisation from THF at −40 °C yielded colourless crystals of **8** (56.8 mg, 95.2 μmol, 48%).

^{1}H NMR (C_6D_6, 400.1 MHz, 26 °C): δ = 9.16 (3H, s, pz-C*H*), 3.78 (18H, s, pz-CH_3), 2.02 (6H, s, NCH_2), 1.58 (9H, s, NCH_3), 0.75 (6H, s, NCH_2) ppm. ^{1}H NMR (toluene-d_8, 400.1 MHz, 26 °C): δ = 9.20 (3H, s, pz-C*H*), 3.79 (18H, s, pz-CH_3), 2.35 (9H, s, NCH_3), 1.76 (6H, s, NCH_2), −0.23 (6H, s, NCH_2) ppm. ^{13}C{^{1}H} NMR (C_6D_6, 100.6 MHz, 26 °C): δ = 161.9 (pz-N*C*), 119.7 (pz-NC*C*H), 46.6 (N*C*H$_2$), 34.0 (N*C*H$_3$), 16.6 (pz-*C*H$_3$) ppm. DRIFT: $\tilde{\nu}$ = 3092 (m), 2969 (s), 2914 (vs), 2872 (s), 2821 (s), 2720 (w), 1512 (s), 1463 (s), 1415 (s), 1368 (m), 1297 (m), 1208 (w), 1152 (w), 1127 (w), 1074 (m), 1043 (m), 1009 (vs), 965 (w), 888 (w), 768 (s), 731 (m), 653 (vw), 571 (w), 499 (vw), 423 (w) cm^{-1}. Elemental analysis (%) calcd for $C_{24}H_{42}CeN_9$ (596.78 g mol^{-1}): C 48.30, H 7.09, N 21.12; found: C 48.51, H 6.96, N 21.22.

Author contributions

J. R.: synthesis and characterisation of compounds, writing and editing the original draft; C. M.-M.: crystallography, editing the original draft; R. A.: conceptualisation, supervision, writing and editing the original draft, project administration, funding acquisition.

Conflicts of interest

There are no conflicts to declare.

Data availability

Data supporting this article have been uploaded as part of the supplementary information (SI). Supplementary information: experimental, spectroscopic and structural data. See DOI: https://doi.org/10.1039/d6dt00453a.

CCDC 2530846–2530850 contain the supplementary crystallographic data for this paper.[65a–e]

Acknowledgements

We are grateful to the VECTOR Foundation (grant P2021-0099) for generous support. We thank Dr Markus Ströbele for performing the TGA experiments, Dr Klaus Eichele for the solid-state NMR measurements and Philipp Wetzel for the VT-NMR experiments.

References

1 P. Falkowski, R. J. Scholes, E. Boyle, J. Canadell, D. Canfield, J. Elser, N. Gruber, K. Hibbard, P. Högberg, S. Linder, F. T. Mackenzie, B. Moore III, T. Pedersen, Y. Rosenthal, S. Seitzinger, V. Smetacek and W. Steffen, The Global Carbon Cycle: A Test of Our Knowledge of Earth as a System, *Science*, 2000, **290**, 291–296.

2 S. Solomon, G.-K. Plattner, R. Knutti and P. Friedlingstein, Irreversible climate change due to carbon dioxide emissions, *Proc. Natl. Acad. Sci. U. S. A.*, 2009, **106**, 1704–1709.

3 R. S. Haszeldine, Carbon Capture and Storage: How Green Can Black Be?, *Science*, 2009, **325**, 1647–1652.

4 D. W. Keith, Why Capture CO_2 from the Atmosphere?, *Science*, 2009, **325**, 1654–1655.

5 Q. Liu, L. Wu, R. Jackstell and M. Beller, Using carbon dioxide as a building block in organic synthesis, *Nat. Commun.*, 2015, **6**, 5933.

6 R. E. Siegel, S. Pattanayak and L. A. Berben, Reactive Capture of CO_2: Opportunities and Challenges, *ACS Catal.*, 2023, **13**, 766–784.

7 M. Aresta, A. Dibenedetto and A. Angelini, Catalysis for the Valorization of Exhaust Carbon: from CO_2 to Chemicals, Materials, and Fuels. Technological Use of CO_2, *Chem. Rev.*, 2014, **114**, 1709–1742.

8 N. von der Assen, P. Voll, M. Peters and A. Bardow, Life cycle assessment of CO_2 capture and utilization: a tutorial review, *Chem. Soc. Rev.*, 2014, **43**, 7982–7994.

9 M. Aresta and A. Dibenedetto, Utilisation of CO_2 as a chemical feedstock: opportunities and challenges, *Dalton Trans.*, 2007, 2975–2992.

10 R. Ayyappan, I. Abdalghani, R. C. Da Costa and G. R. Owen, Recent developments on the transformation of CO_2 utilising ligand cooperation and related strategies, *Dalton Trans.*, 2022, **51**, 11582–11611.

11 J. Hack, N. Maeda and D. M. Meier, Review on CO_2 Capture Using Amine-Functionalized Materials, *ACS Omega*, 2022, **7**, 39520–39530.

12 U. Bayer, D. Werner, C. Maichle-Mössmer and R. Anwander, Effective and Reversible Carbon Dioxide Insertion into Cerium Pyrazolates, *Angew. Chem., Int. Ed.*, 2020, **59**, 5830–5836.

13 F. Kracht, P. Rolser, P. Preisenberger, C. Maichle-Mössmer and R. Anwander, Organomagnesia: Reversibly High Carbon Dioxide Uptake by Magnesium Pyrazolates, *Adv. Sci.*, 2024, **11**, 2403295.

14 F. Kracht, P. Rolser, K. Eichele, C. Maichle-Mössmer and R. Anwander, Carbon dioxide affinity ("carboxophilicity") of trivalent light metal pyrazolates, *Inorg. Chem. Front.*, 2024, **11**, 6948–6959.

15 F. Kracht, S. Mayer, C. Maichle-Mössmer and R. Anwander, Reactivity of titanium pyrazolates towards CO_2, CS_2 and N_2O, *Dalton Trans.*, 2025, **54**, 10890–10897.

16 F. G. Bordwell, Equilibrium acidities in dimethyl sulfoxide solution, *Acc. Chem. Res.*, 1988, **21**, 456–463.

17 T. M. Klapötke, *Chemistry of High-Energy Materials*, De Gruyter, Berlin, Boston, 7th edn, 2025.

18 K. Müller-Buschbaum and Y. Mokaddem, Three-dimensional networks of lanthanide 1,2,4-triazolates: $^3{}_\infty$[Yb(Tz)$_3$] and $^3{}_\infty$[Eu$_2$(Tz)$_5$(TzH)$_2$], the first 4f networks with complete nitrogen coordination, *Chem. Commun.*, 2006, 2060–2062.

19 K. Müller-Buschbaum, Y. Mokaddem and C. J. Höller, On an Unexpected 2D-linked Rare Earth 1,2,4-Triazolate Network: Synthesis, Crystal Structure, Spectroscopic and

Thermal Properties of $^{2}_{\infty}[Ho(Tz)_3(TzH)_2]TzH$, *Z. Anorg. Allg. Chem.*, 2008, **634**, 2973–2977.

20 Y.-L. Wang, M. Feng, X. Tao, Q.-Y. Tang and Y.-Z. Shen, Two lanthanum(III) complexes containing η^2-pyrazolate and η^2-1,2,4-triazolate ligands: intramolecular C-H...N/O interactions and coordination geometries, *Acta Crystallogr., Sect. C: Cryst. Struct. Commun.*, 2013, **69**, 25–28.

21 P.-H. Guo, Y. Meng, Y.-C. Chen, Q.-W. Li, B.-Y. Wang, J.-D. Leng, D.-H. Bao, J.-H. Jia and M.-L. Tong, A zigzag Dy^{III}_4 cluster exhibiting single-molecule magnet, ferroelectric and white-light emitting properties, *J. Mater. Chem. C*, 2014, **2**, 8858–8864.

22 H. Yang, F. Cao, D. Li, S. Zeng, Y. Song and J. Dou, A Family of 12-Azametallacrown-4 Structural Motif with Heterometallic Mn^{III}-Ln-Mn^{III}-Ln (Ln=Dy, Er, Yb, Tb, Y) Alternate Arrangement and Single-Molecule Magnet Behavior, *Chem. – Eur. J.*, 2015, **21**, 14478–14485.

23 J. C. Rybak, L. V. Meyer, J. Wagenhöfer, G. Sextl and K. Müller-Buschbaum, Homoleptic Lanthanide 1,2,3-Triazolates $^{2-3}_{\infty}[Ln(Tz^*)_3]$ and Their Diversified Photoluminescence Properties, *Inorg. Chem.*, 2012, **51**, 13204–13213.

24 K. Müller-Buschbaum and Y. Mokaddem, MOFs by solvent free high temperature synthesis exemplified by $^{3}_{\infty}[Eu_3(Tz^*)_6(Tz^*H)_2]$, *Solid State Sci.*, 2008, **10**, 416–420.

25 J.-C. Rybak, M. Tegel, D. Johrendt and K. Müller-Buschbaum, Polymorphism of isotypic series of homoleptic 1,2,3-triazolate MOFs $[Ln(Tz^*)_3]$ containing the heavy lanthanides Gd–Lu: from open to dense frameworks of varying dimensionality, *Z. Kristallogr. – Cryst. Mater.*, 2010, **225**, 187–194.

26 K. Müller-Buschbaum and Y. Mokaddem, Rare Earth Benzotriazolates: Coordination Polymers Incorporating Decomposition Products from Ammonia to 1,2-Diaminobenzene in $^{1}_{\infty}[Ln(Btz)_3(BtzH)]$ (Ln = Ce, Pr), $^{1}_{\infty}[Ln(Btz)_3\{Ph(NH_2)_2\}]$ (Ln = Nd, Tb, Yb), and $^{1}_{\infty}[Ho_2(Btz)_6(BtzH)(NH_3)]$, *Eur. J. Inorg. Chem.*, 2006, **2006**, 2000–2010.

27 J. Chu, C. E. Kefalidis, L. Maron, X. Leng and Y. Chen, Chameleon Behavior of a Newly Synthesized Scandium Nitrilimine Derivative, *J. Am. Chem. Soc.*, 2013, **135**, 8165–8168.

28 W. J. Evans, E. Montalvo, T. M. Champagne, J. W. Ziller, A. G. DiPasquale and A. L. Rheingold, Organolanthanide-Based Synthesis of 1,2,3-Triazoles from Nitriles and Diazo Compounds, *J. Am. Chem. Soc.*, 2008, **130**, 16–17.

29 J. Riedmaier, C. Maichle-Mössmer and R. Anwander, Cerium(III) Azolate Promoted CO_2 Insertion, *Inorg. Chem.*, 2025, **64**, 22238–22250.

30 P. C. Andrews, P. C. Junk, M. Massi and M. Silberstein, Gelation of La(III) cations promoted by 5-(2-pyridyl)tetrazolate and water, *Chem. Commun.*, 2006, 3317–3319.

31 P. J. Eulgem, A. Klein, N. Maggiarosa, D. Naumann and R. W. H. Pohl, New Rare Earth Metal Complexes with Nitrogen-Rich Ligands: 5,5′-Bitetrazolate and 1,3-Bis(tetrazol-5-yl)triazenate—On the Borderline between Coordination and the Formation of Salt-Like Compounds, *Chem. – Eur. J.*, 2008, **14**, 3727–3736.

32 D. Werner, U. Bayer, N. E. Rad, P. C. Junk, G. B. Deacon and R. Anwander, Unique and contrasting structures of homoleptic lanthanum(III) and cerium(III) 3,5-dimethylpyrazolates, *Dalton Trans.*, 2018, **47**, 5952–5955.

33 Z. Guo, J. Luu, V. Blair, G. B. Deacon and P. C. Junk, Replacing Mercury: Syntheses of Lanthanoid Pyrazolates from Free Lanthanoid Metals, Pentafluorophenylsilver, and Pyrazoles, Aided by a Facile Synthesis of Polyfluoroarylsilver Compounds, *Eur. J. Inorg. Chem.*, 2019, **2019**, 1018–1029.

34 D. Barisic, D. Diether, C. Maichle-Mössmer and R. Anwander, Trimethylscandium, *J. Am. Chem. Soc.*, 2019, **141**, 13931–13940.

35 C. S. Tredget, S. C. Lawrence, B. D. Ward, R. G. Howe, A. R. Cowley and P. Mountford, A Family of Scandium and Yttrium Tris((trimethylsilyl)methyl) Complexes with Neutral N_3 Donor Ligands, *Organometallics*, 2005, **24**, 3136–3148.

36 E. Curnock, W. Levason, M. E. Light, S. K. Luthra, G. McRobbie, F. M. Monzittu, G. Reid and R. N. Williams, Group 3 metal trihalide complexes with neutral N-donor ligands – exploring their affinity towards fluoride, *Dalton Trans.*, 2018, **47**, 6059–6068.

37 S. Hajela, W. P. Schaefer and J. E. Bercaw, Highly electron deficient group 3 organometallic complexes based on the 1,4,7-trimethyl-1,4,7-triazacyclononane ligand system, *J. Organomet. Chem.*, 1997, **532**, 45–53.

38 J. Lebon, C. Maichle-Mössmer and R. Anwander, Putting on the Crown: Synthesis and Reactivity of Trimethyltitanium, *Organometallics*, 2023, **42**, 1386–1394.

39 A. Mortis, C. Maichle-Mössmer and R. Anwander, Mixed Methyl/Chlorido Yttrium(III) Complexes Supported by a Neutral Tridentate N-Donor Ligand, *Organometallics*, 2023, **42**, 1158–1165.

40 J. C. Wedal, J. W. Ziller and W. J. Evans, Trimethyltriazacyclohexane coordination chemistry of simple rare-earth metal salts, *Dalton Trans.*, 2023, **52**, 4787–4795.

41 S. Bambirra, A. Meetsma and B. Hessen, An octahedrally coordinated trialkylyttrium(III): tris(trimethylsilylmethyl)(1,4,7-trimethyl-1,4,7-triazacyclononane)yttrium(III), *Acta Crystallogr., Sect. E: Struct. Rep. Online*, 2006, **62**, m314–m316.

42 A. Mortis, C. Maichle-Mössmer and R. Anwander, Yttrium tris(trimethylsilylmethyl) complexes grafted onto MCM-48 mesoporous silica nanoparticles, *Dalton Trans.*, 2022, **51**, 1070–1085.

43 S. Bambirra, A. Meetsma and B. Hessen, Tris(4-methylbenzyl)(1,4,7-trimethyl-1,4,7-triazacyclononane)lanthanum(III), *Acta Crystallogr., Sect. E: Struct. Rep. Online*, 2007, **63**, m2891.

44 D. A. Bardonov, P. D. Komarov, V. I. Ovchinnikova, L. N. Puntus, M. E. Minyaev, I. E. Nifant'ev, K. A. Lyssenko, V. M. Korshunov, I. V. Taidakov and D. M. Roitershtein,

Accessing Mononuclear Triphenylcyclopentadienyl Lanthanide Complexes by Using Tridentate Nitrogen Ligands: Synthesis, Structure, Luminescence, and Catalysis, *Organometallics*, 2021, **40**, 1235–1243.

45 G. I. Sadrtdinova, D. A. Bardonov, K. A. Lyssenko, M. E. Minyaev, I. E. Nifant'ev and D. M. Roitershtein, (Cyclopentadienyl)neodymium borohydrides with auxiliary N_3-heterocyclic ligands, *Mendeleev Commun.*, 2023, **33**, 357–359.

46 S. S. Degtyareva, D. A. Bardonov, K. A. Lysenko, M. E. Minyaev, I. E. Nifant'ev and D. M. Roitershtein, Lanthanide Complexes with 1,4,7-Trimethyl-1,4,7-triazacyclononane, *Russ. J. Coord. Chem.*, 2024, **50**, 292–299.

47 A. Mortis, C. Maichle-Mössmer and R. Anwander, Distinct Reactivity of Trimethylytterbium toward $AlMe_3$ and $GaMe_3$: Synthesis of Donor-Stabilized Dimethylytterbium, *Chem. – Eur. J.*, 2023, **29**, e202203824.

48 J. P. Stiel, J. W. Ziller and W. J. Evans, On the Use of $Ce[N(SiMe_3)_2]_3(THF)_n$ in Catalysis, *Inorg. Chem.*, 2025, **64**, 23345–23347.

49 D. Müller, C. Knoll, A. Herrmann, G. Savasci, J. M. Welch, W. Artner, J. Ofner, B. Lendl, G. Giester, P. Weinberger and G. Steinhauser, Azobis[tetrazolide]-Carbonates of the Lanthanides – Breaking the Gadolinium Break, *Eur. J. Inorg. Chem.*, 2018, **2018**, 1969–1975.

50 D.-X. Xue, A. J. Cairns, Y. Belmabkhout, L. Wojtas, Y. Liu, M. H. Alkordi and M. Eddaoudi, Tunable Rare-Earth fcu-MOFs: A Platform for Systematic Enhancement of CO_2 Adsorption Energetics and Uptake, *J. Am. Chem. Soc.*, 2013, **135**, 7660–7667.

51 Y. A. Belousov, V. E. Goncharenko, A. M. Lunev, A. V. Sidoruk, S. I. Bezzubov and I. V. Taidakov, New Heteroligand Europium and Gadolinium Formate Triazole Dicarboxylates: Synthesis, Structures, and Luminescence Properties, *Russ. J. Coord. Chem.*, 2020, **46**, 394–401.

52 F. Kracht and R. Anwander, Light metal pyrazolates excel in carbon dioxide uptake, *Chem. Commun.*, 2026, **62**, 5588–5602.

53 M. I. Anwar, M. Asad, X. Su, Z. Sofer, M. S. Rabbani, M. N. Ashiq, G. Yang and Y. Gao, Azolate-based metal-organic frameworks and derivatives for electrochemical CO_2 reduction reactions: Recent advances and perspectives, *Coord. Chem. Rev.*, 2026, **548**, 217158.

54 D. C. Bradley, J. S. Ghotra and F. A. Hart, Low coordination numbers in lanthanide and actinide compounds. Part I. The preparation and characterization of tris{bis(trimethylsilyl)-amido}lanthanides, *J. Chem. Soc., Dalton Trans.*, 1973, 1021–1023.

55 *COSMO, v 1.61*, Bruker AXS Inc., Madison, WI, 2012.

56 *APEX 3, v. 2019.11-0*, Bruker AXS Inc., Madison, WI, 2019.

57 *SAINT, v. 8.38B*, Bruker AXS Inc., Madison, WI, 2019.

58 L. Krause, R. Herbst-Irmer, G. M. Sheldrick and D. Stalke, Comparison of silver and molybdenum microfocus X-ray sources for single-crystal structure determination, *J. Appl. Crystallogr.*, 2015, **48**, 3–10.

59 G. M. Sheldrick, *SHELXT* – Integrated space-group and crystal-structure determination, *Acta Crystallogr., Sect. A*, 2015, **71**, 3–8.

60 G. M. Sheldrick, Crystal structure refinement with *SHELXL*, *Acta Crystallogr., Sect. C*, 2015, **71**, 3–8.

61 D. Kratzert, J. J. Holstein and I. Krossing, *DSR*: enhanced modelling and refinement of disordered structures with *SHELXL*, *J. Appl. Crystallogr.*, 2015, **48**, 933–938.

62 C. B. Hübschle, G. M. Sheldrick and B. Dittrich, *ShelXle*: a Qt graphical user interface for *SHELXL*, *J. Appl. Crystallogr.*, 2011, **44**, 1281–1284.

63 C. F. Macrae, I. J. Bruno, J. A. Chisholm, P. R. Edgington, P. McCabe, E. Pidcock, L. Rodriguez-Monge, R. Taylor, J. van de Streek and P. A. Wood, *Mercury CSD* 2.0 - new features for the visualization and investigation of crystal structures, *J. Appl. Crystallogr.*, 2008, **41**, 466–470.

64 *POV Ray*, V. 3.6; Williamstown, Victoria, Australia, 2004, https://www.povray.org.

65 (*a*) CCDC 2530846: Experimental Crystal Structure Determination, 2026, DOI: 10.5517/ccdc.csd.cc2qyk6g; (*b*) CCDC 2530847: Experimental Crystal Structure Determination, 2026, DOI: 10.5517/ccdc.csd.cc2qyk7h; (*c*) CCDC 2530848: Experimental Crystal Structure Determination, 2026, DOI: 10.5517/ccdc.csd.cc2qyk8j; (*d*) CCDC 2530849: Experimental Crystal Structure Determination, 2026, DOI: 10.5517/ccdc.csd.cc2qyk9k; (*e*) CCDC 2530850: Experimental Crystal Structure Determination, 2026, DOI: 10.5517/ccdc.csd.cc2qykbl.